EFFECTIVENESS AND OPTIMIZATION OF FIBER BRAGG GRATING SENSOR AS EMBEDDED STRAIN SENSOR

Xiaoming Tao[1], Liqun Tang[1,3], Chung-Loong Choy[2]

[1]Institute of Textiles and Clothing, [2]Materials Research Centre,
The Hong Kong Polytechnic University
[3]Dept. of Engineering Mechanics, Traffic and Communications College,
South China University of Technology

SUMMARY: The strain field of a host with an embedded optic fiber is analyzed under a uniform three-principal strain load on the host in order to study the measurement effectiveness of fiber Bragg grating sensor (FBGS) as embedded strain sensor. Three indicators are defined to depict the strain measurement effectiveness of a fiber Bragg grating sensor embedded in a host. The numerical results represent the strain distributions in the host, coating and optic fiber as functions of the elastic modulus of coating and the geometrical parameters of the host. The effects of these parameters on the measurement effectiveness indicators are also studied and the optimal values of these parameters are suggested.

KEYWORDS: fiber Bragg grating sensor, effectiveness, optimization, smart materials

1. INTRODUCTION

The fiber Bragg grating sensors (FBGSs) now have attracted more and more attention as embedded sensors to monitor or measure the internal strain of composite structures [1-6]. By using FBGS, the strain is determined by measuring the shift of the Bragg wavelength of the reflective wave peak from the gratings in the optic fiber, $\Delta\lambda$, which is directly related with the axial strain, ε_1, of the optic fiber. When embedded in a host, the FBGS can be used to measure the internal strain of the host.

Previous analysis [3-5] showed that the sensitivity factor f between $\Delta\lambda$ and ε_1 is not a constant but a function of the ratio of the transverse strain over the axial strain. Without considering temperature effect, the relationship can be expressed below:

$$\frac{\Delta\lambda}{\lambda} = f\varepsilon_1 \tag{1}$$

and

$$f = 1 - \frac{n^2}{2}[P_{12} + (P_{11} + P_{12})\upsilon^*] \ , \ \upsilon^* = \frac{\varepsilon_2}{\varepsilon_1} \tag{2}$$

where ε_2 is the transverse strain of the optic fiber when the strains in the two transverse directions are uniform; P_{11}, P_{12} are the strain-optic constants of optic fiber; and υ^* is the effective Poisson ratio (EPR).

If there is no restriction in the transverse direction of the optic fiber, thus υ^* is equal to the Poisson ratio (PR) υ of the fiber, then f is a constant which has the value recommended by many FBGS's manufacturers. However when embedded in a host, an optic fiber may be subjected to force/deformation in its transverse directions. The effective Poisson ratio, υ^*, may not be taken as the Poisson ratio of optic fiber or even a constant [5].

One may assume that the optic fiber's axial strain is equal to that of host in the optic fiber direction, which implies that the presence of the embedded FBGS has no or little effect on the strain distribution of the host and what the sensor measures should be the strain of the host without the sensor. In real situations, therefore, there are three issues critical to the measurement effectiveness of an embedded FBGS: (1)whether the effect of embedded optic fiber on the initial host strain field is negligible; (2) whether the optic fiber's axial strain is close enough to that of host in the optic fiber axial direction; and (3) whether EPR υ^* can be regarded as a constant during the measurement. If EPR is a constant but not equal to υ, it is necessary to calibrate the sensor in order to determine the value of f after it is embedded into a host.

Many authors studied the stress concentration induced by the embedded fiber optic sensors [7-12] where the optimal parameters, such as the coating's modulus and thickness, were considered for the reduction of the concentration in the fiber cross section plane. Most of the questions on the measurement effectiveness remain unanswered. Hence, this paper is intended to address the three issues of the measurement effectiveness of embedded FBGS for both the axial and transverse strains.

2. THREE-LAYER COMPOSITE AND NUMERICAL MODELING

A case study was conducted by applying a uniform three-principal load to a host with embedded fiber sensor, then examining the measurement effectiveness of embedded FBGS by solving the strain field of the composite comprising host, coating and optic fiber. For a homogenous and isotropic material, the simple way to apply a uniform three principal load on the material is to apply a thermal load on it, and the principal strain of the material is equal to the thermal expansionary strain. Here it is should be emphasized that the thermal load is applied to the host only.

The optic-fiber-host system can be illustrated as a composite comprising a cylindrical fiber and two concentric shell layers, with fiber, coating and host arranged from the center to the out surface (Fig.1). The height of the composite cylinder is $2H$, the radius of fiber is R_1, which is also the inter radius of coating, R_2 is the outer radius of coating and the inter radius of host, R_3 is the out radius of the host. The following basic assumptions have been made so that the case can be simplified as an axial-symmetric problem: (1) The optical fiber, coating of fiber and host are linear elastic and isotropic; (2) The thermal expansion coefficients of fiber, coating and host are constants; (3) There is no discontinuity in the displacements at the interfaces of fiber and coating, coating and host under the loading condition; (4) Thermal load is uniform in the whole cylindrical shell host.

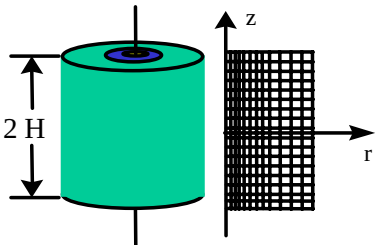

Fig. 1: Geometry and FE model of the three-layered composite.

The finite element (FE) analysis was applied by using a commercial program ABAQUS. Four-node bilinear elements (CAX4) were used to generate meshes. Because of the symmetry to the r axis, only half of the cylinder was considered for the strain analysis. The boundary conditions are $u\big|_{r=0}=0$ and $v\big|_{z=0}=0$, where u, v are the displacements along the r, z direction respectively. The material constants and dimensions are listed in Table 2:

Table 1: The material constants and dimensions used for computation

Parameter	Fiber	Coating	Host
E (GPa)	72.9	0.045-72.9, 0.045*	49.
υ	0.17	0.34	0.288
α (10^{-6}/ ^{0}C)	0	0	13.38
R_1 (mm)	0.063		
R_2 (mm)	0.123		
R_3 (mm)	0.3-10, 1.0*		
H (mm)	10-90, 10*		

E, υ and α are the elastic modulus, Poisson's ratio and thermal expansion coefficient respectively, subscripts "h", "c", "f" represent fiber, coating and host, respectively. The host parameters are those of polyester. The values with "*" are the default values, some of them were provided by commercial suppliers.

3. NUMERICAL RESULTS AND ANALYSIS

A thermal load of ΔT =25^{0}C was applied to the host only. Without the embedded fiber, the strain field should be uniform in the host and equal to:

$$\varepsilon_0 = \alpha_h \times \Delta T = 0.000325 \tag{3}$$

The strain in the fiber axial direction, ε_1, is the most important term in our discussion and its normalized term, e, will be used in the rest of this section unless stated, which is given by:

$$e = \varepsilon_1 / \varepsilon_0 \tag{4}$$

3.1 Distributions of normalized strain and EPR

Figures 2, 3 and 4 illustrate the normalized strain distributions in the fiber, host and coating, respectively. The strains, calculated by using the default values in Table 1, are in the fiber axial direction and expressed as functions of radius r as well as the composite half height z. Fig.2 shows that the normalized strain of fiber declines with the increasing length z. As the middle part of the optic fiber is restricted more than the parts near two ends, the strain of middle optic fiber is closer to that of the host without embedded fiber sensor (e = 1). The

strain distribution curves are identical regardless the radial position in the fiber, thus the strain of fiber can be regarded as a function of z only.

Fig.3 shows reverse trends of strain distribution in the host along the height direction. The strain level of the middle host is lower than that of the host near the boundary, which is because the middle host is restricted more by the fiber and the hosts near boundary can expanse more freely under a thermal load. The normalized strain values of the host are very close to 1 ($0.995 < e < 1$), which implies that the host with embedded fiber sensor has a strain field very close to that without embedded optic fiber. Because of its lower elastic modulus in this case, the strain distribution of the coating is significantly affected by both the

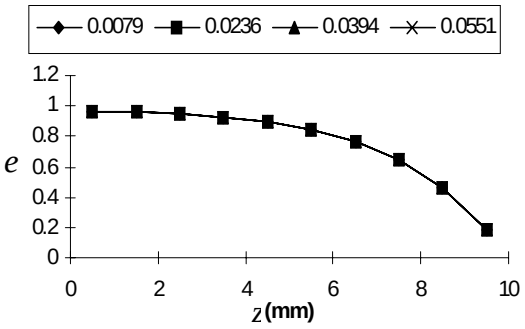

Fig.2 Distribution of fiber's axial strain .

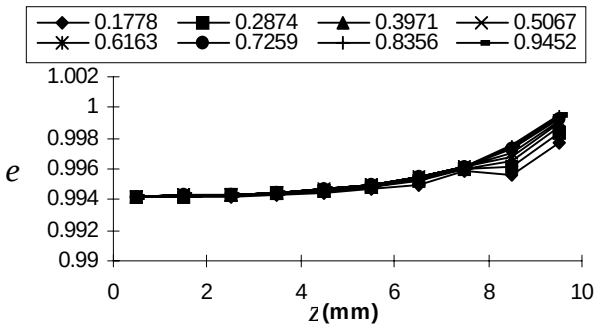

Fig.3 Distribution of host's axial strain .

fiber and host, as shown in Fig.4. The strain distribution along the z is similar with that of the fiber when r approaches R_1, and the strain near the outer surface of coating varies little along z like that of host. The distribution of EPR is shown in Fig.5, where EPR, υ^*, is plotted against z with r as a parameters. The EPR has little variation inside of the optic fiber.

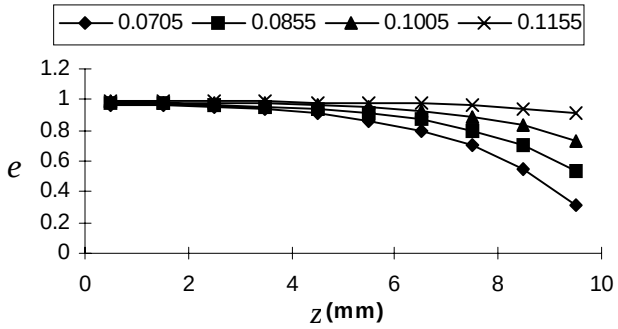

Fig.4: Distribution of coating's axial strain.

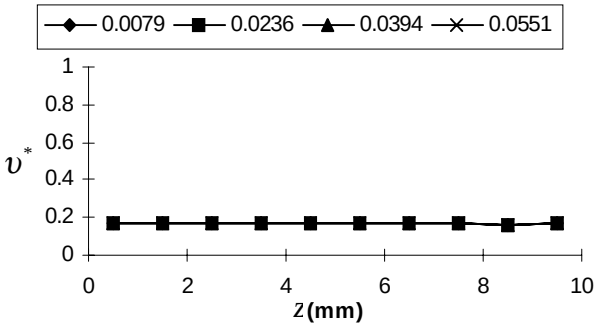

Fig.5: Distribution of fiber's effective Poisson's ratio along the fiber length.

3.2 Three indicators of the measurement effectiveness of FBGS

In order to depict the three issues of the measurement effectiveness quantitatively, in this section, we will introduce three indicators. The max relative error $R_{\max}$, the effective fiber-host strain ratio β, and the effective Poisson's ratio EPR-PR ratio υ_0 are defined as follow:

(1) Max relative error $R_{\max}$ is defined as the maximum relative error of the strain of the host

with embedded fiber with respect to that without embedded fiber, i.e.:

$$R_{\max} = \mathrm{Max}\left(\left|\frac{\varepsilon_1 - \varepsilon_0}{\varepsilon_0}\right|\right) \tag{5}$$

(2) Because the axial strain of optic fiber is uniform in its cross section, as discussed in Section 3.1, let e_f be the fiber axial strain, e_h^{in} be the host strain near the coating, then the fiber-host strain ratio can be defined as:

$$S_{fh} = \frac{e_f}{e_h^{in}} \tag{6}$$

However, S_{fh} varies significantly along z (Fig. 6) with a similar trend to the fiber's axial strain. Hence we use a height H_{95} where the S_{fh} declines to 0.95. The physical meaning of H_{95} is that only within the range of $|z| < H_{95}$ the strain of optic fiber can represent that of host effectively, with a maximum difference of 5%. Using this height, now the new fiber-host strain ratio β is defined by:

$$\beta = \frac{H_{95}}{H} \tag{7}$$

β reflects the proportion of an optic fiber inside of host suitable for sensing within the specified maximum difference of 5%.

(3) Because the EPR varies little along z, as shown in Figure 5, we simply define the ratio of the effective Poisson's ratio to Poisson's ratio (EPR-PR ratio) υ_0 as the EPR at z =0 over the Poisson's ratio of the fiber , i.e.:

$$\upsilon_0 = \frac{\upsilon^*(z=0)}{\upsilon} \tag{8}$$

Following the definitions of $R_{\max}$, β and υ_0, an effective embedded FBGS demands lower values of $R_{\max}$ as well as higher values of β and υ_0.

3.3 Factors influencing the measurement effectiveness indicators

Three factors have been investigated including the coating elastic modulus E_c, host's thickness (related R_3) and height H of host (length of optic fiber inside host).

In order to obtain a completed picture of their effects on the effectiveness indicators and to identify the optimal values of parameters, we let the three factors vary in their own ranges as listed in Table 1.

Furthermore, the effect of the host elastic modulus E_h on the effectiveness is examined with other parameters taking default values.

Fig.6 Distribution of fibre strain ratio along fibre length.

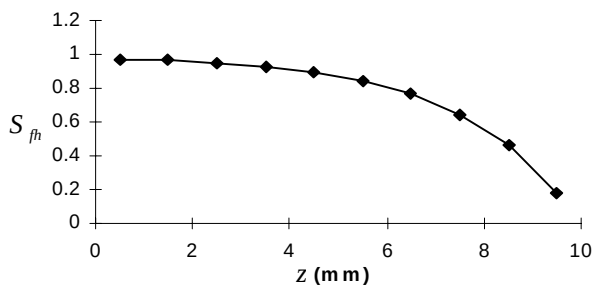

3.3.1 Maximum relative error R_{max}

The numerical analysis indicate that the maximum relative error R_{max} is not sensitive to the host's length H (>10 cm), when the host out radius R_3 >0.3 mm. An example can be seen in Fig.7 with R_3 taking the default value of 1 mm. R_{max} increases with the elastic modulus of coating gradually, and declines rapidly with increment of the thickness of host especially when the host is thin (Fig.8).

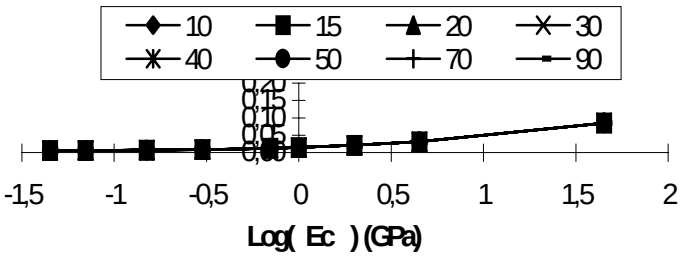

Fig.7 : Maximum relative error.

While E_c takes its default value (0.045GPa), with R_3 >1mm, the maximum relative error is smaller than 1%. When E_c reaches 1 GPa, with R_3 >0.7mm, R_{max} is still smaller than 2%. Therefore it cam be concluded that the influence of optic fiber on the host strain field is small and can be negligible in general cases.

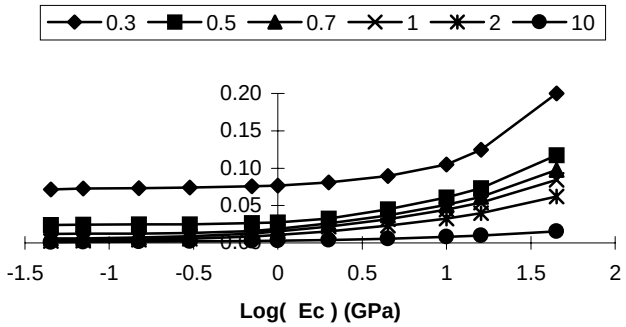

Fig.8 : Maximum relative error.

3.3.2 Fiber-host strain ratio β

β is independent of the host's thickness (R_3 >0.3). An example can be seen in Fig.9 with H taking the default value. β increases with the increment in coating elastic modulus E_c or host's height H , as shown in Figure 10. E_c =1 GPa seems a threshold value because after that point the curves reach their plateau and the effect of E_c on β becomes very small. The threshold value is β >0.85 for all the heights, H > 10 mm, under the current investigation. If the default value E_c =0.045 GPa is chosen, the height H has to be more than 50 mm to ensure β >0.85.

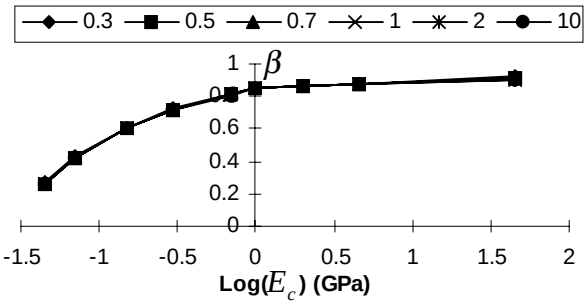

Fig.9: Fiber-host strain ratio against the coating elastic modulus with outer radius of host as a parameter.

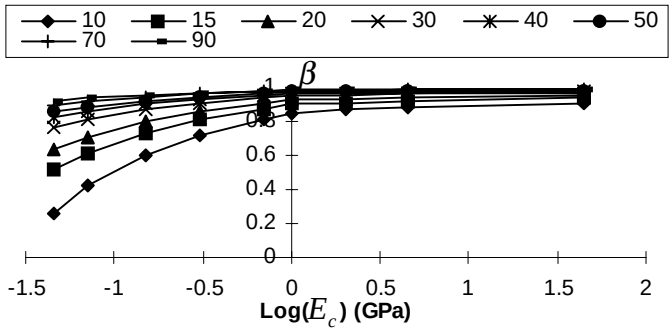

Fig.10: Fiber-host strain ratio against the coating elastic modulus with height of host as a parameter.

3.3.3 EPR-PR ratio υ_0

Having a similar property to that of fiber-host strain ratio β, υ_0 decreases as the coating elastic modulus increases but it has a small relation with the host's thickness ($R_3 \geq 0.3$) when $H > 10$ mm. An example can be seen in Fig.11 with the default values. υ_0 declines with the increment of the coating elastic modulus E_c. The larger E_c causes more coupling of the host's strain into the transverse strain of optic fiber, however, the curve varies gently when $E_c \leq 1$GPa. The difference between the curves become larger when $E_c > 1$GPa. Then the small effects of R_3 and H on υ_0 become visible (Fig.11, Fig.12).

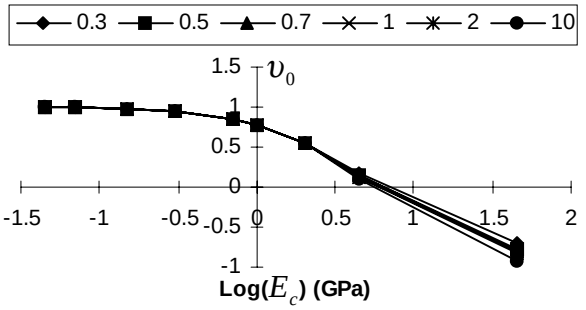

Fig.11: EPR-PR ratio against the coating elastic modulus with outer radius of host as a parameter.

From Figure 12, with a default value of E_c=0.045 GPa, υ_0=1. This implies that there is no host's strain to be coupled into the fiber's transverse strain even the host's transverse strain has the same quantity as the fiber axial strain. Therefore, we can use the value of sensitivity factor f, derived from the theoretical prediction, in our measurement without correction.

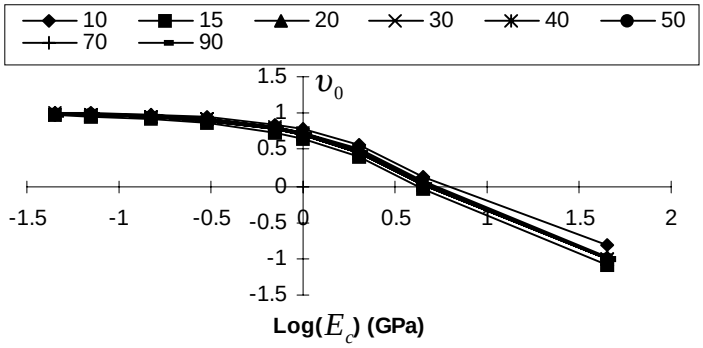

Fig.12: EPR-PR ratio against the coating elastic modulus with height of host as a parameter.

From Eqn 2, we can derive two special cases as follow:

(1) No strain coupling: $\upsilon^* = \upsilon$, $f = 0.798$,

(2) With strain coupling: $\upsilon^* = \upsilon_0 \times \upsilon$ =0.132, $f = 0.783$

where from Figure 12, if E_c =1 GPa, and H =10 mm, then υ_0 = 0.776. The material properties of optic fiber are given in Table 2.

Table 2: Material parameters of optic fiber.

Strain-optic coefficient		Index of refraction	Elastic modulus	Poisson's ratio
P_{11}	P_{12}	n	E (GPa)	υ
0.113	0.252	1.458	70	0.17

The relative error between the factor with and without strain coupling is smaller than 2%. Therefore E_c =1 GPa is a good threshold value for all the three indicators of the measurement effectiveness, that is, $R_{\max}$, β, and υ_0. However if E_c = 45Gpa, which is the same as that of the host, then $\upsilon_0 = -1$, according to Fig,12. The sensitivity factor f is equal to 0.666. In this case how to calibrate the sensor after it is embedded into the host becomes an important problem. In practice, it is very difficult to use the coating with such high elastic modulus. But sometimes, the host may permeate into the coating during the procedure of embedding the sensor when the host is in state of liquid (such as polyester, epoxy), which will increase the coating's elastic modulus evidently.

4. CONCLUSION

The present numerical analysis on the strain field of the three-layer composite comprising a host with an embedded optic fiber draws some conclusions as follow:

(1) A thick host and a large embedded length of an optic fiber will improve the measurement effectiveness of the embedded optic sensor.

(2) A high elastic modulus E_c of coating is beneficial for improving the effective fiber-host strain ratio β, but this positive effect is count-balanced by a high value of the maximum

relative error and a large variation in the EPR-PR ratio υ_0 value. By considering the three effectiveness indicators together, an optimal value of the coating elastic modulus, E_c=1Gpa, is recommended to achieve the optimal measurement performance of FBGS.

(3) Should the host resin permeate into the coating during the embedding procedure, the coating elastic modulus of FBGS might increase significantly and the FBGS would be used in a complicated stress status. Care should be taken to choose the suitable value of the sensitivity factor f, or it might be necessary to calibrate the embedded FBGS .

(4) Within the range of the default parameters used, the effect of embedded FBGS on the initial strain field of a host is negligible, except that the host's diameter is very small (compatible with that of coating). The strain of FBGS cannot represent that of the host section in which the fiber is embedded, only at the portion far away from the boundary of host is suitable for the measurement. The longer the embedded FBGS is, the larger proportion of the usable portion of the fiber. The default value of sensitivity factor f can be used in this case.

Acknowledgments

We would like to acknowledge the Hong Kong University Research Grant Council for supporting this work, which was carried out at the Hong Kong Polytechnic University.

References

1. Du W. C., Tao X. M., Tam H. Y., Choy C. L. Optical Fiber Bragg Grating Sensors In Smart Textile Structural Composite. *Proceedings of the 4th International Conference on Composite Engineering, ICCE/4*, Hawaii, USA, 1997, 289-290.
2. Eric Udd. Fiber Optic Sensor Overview. *Fiber Optic Smart Structures*, Ed: Eric Udd, John Wiley & Sons Inc, 1995.
3. Measures R. M. Fiber Optic Strain Sensing. *Fiber Optic Smart Structures*, Ed: Eric Udd, John Wiley & Sons Inc, 1995.
4. Jackson D. A., Jones J.D.C. Fibre Optic Sensors. *Pot Acta* 1986, **33**, 1469-1503.
5. Tao X. M., Tang L. Q., Du W. C., Choy C. L. Internal strain measurment by fiber Bragg grating sensors in textile composites. Submitted to J Composite Science and Technology
6. Butter C. D., Hocker G P. Fiber Optics Strain Gauge. *Appl Opt*, 1992, **1370**, 189-196.
7. Sirkis J. S., Dasgupta A. Optimal Coating for Intelligent Structure Fiber Optical Sensors. *Proceedings of the SPIE*, 1990, **1370**, 129-134.
8. Pak Y. E., DyReyes V., Schmuter E. S. Micromechanics of Fiber Optic Sensors. *Proceedings of the ADPA/AIAA/ASME/ SPIE Conference*, 1992, 121-128.
9. Madsen J. S., Jardine A. P., Meilunas R. J., Tobin A, Pak Y E. Effect of Coating Characteristics on Strain Transfer In Embedded Fiber-Optic Sensors. *Proceedings of the SPIE*, 1993, **1918**, 228-236.
10. Hadjiprocopiou M., Reed G. T., Hollaway L., Thorne A. M. Optimisation of Coating Properties for Fibre Optic Smart Structures Using Finite Element Analysis. *Proceedings of the SPIE*, 1995, **2442**, 109-120.
11. Hadjiprocoplou M., Reed G. T., Hollaway L, Thorne A M. Optimization of Fibre Coating Properties for Fiber Optic Smart Structures. *Smart Materials and Structures*, 1996, **5**(4), 441-448.
12. Levin K., Nilsson S. Analysis of the Local Stress Field an a Composite Material with an Embedded EFPI-Sensor. *Proceedings of the SPIE*, 1994, **2361**: 379-382.